

Deep Galaxy Counts, Extragalactic Background Light, and the Stellar Baryon Budget

Piero Madau^{1,2} and Lucia Pozzetti³

ABSTRACT

We assess the constraints imposed by the observed extragalactic background light (EBL) on the cosmic history of star formation and the stellar mass density today. The logarithmic slope of the galaxy number-magnitude relation from the *Southern Hubble Deep Field* imaging survey is flatter than 0.4 in all seven *UBVIJHK* optical bandpasses, i.e. the light from resolved galaxies has converged from the UV to the near-IR. We find a lower limit to the surface brightness of the optical extragalactic sky of about $15 \text{ nW m}^{-2} \text{ sr}^{-1}$, comparable to the intensity of the far-IR background from *COBE* data. Assuming a Salpeter initial mass function with a lower cutoff consistent with observations of M subdwarf disk stars, we set a lower limit of $\Omega_{g+s} h^2 > 0.0013 I_{50}$ to the visible (processed gas + stars) mass density required to generate an EBL at a level of $50 I_{50} \text{ nW m}^{-2} \text{ sr}^{-1}$; our ‘best-guess’ value is $\Omega_{g+s} h^2 \approx 0.0031 I_{50}$. Motivated by the recent microlensing results of the MACHO collaboration, we consider the possibility that massive dark halos around spiral galaxies are composed of faint white dwarfs, and show that only a small fraction ($\lesssim 5\%$) of the nucleosynthetic baryons can be locked in the remnants of intermediate-mass stars forming at $z_F \lesssim 5$, as the bright early phases of such halos would otherwise overproduce the observed EBL.

Subject headings: cosmology: miscellaneous – dark matter – diffuse radiation – galaxies: evolution – Galaxy: halo

1. Introduction

Recent progress in our understanding of faint galaxy data made possible by the combination of *Hubble Space Telescope* (*HST*) deep imaging and ground-based spectroscopy has vastly improved our understanding of the evolution of the stellar birthrate in optically-selected galaxies from the present-epoch up to $z \approx 4$ (Steidel et al. 1998; Madau et al. 1998; Ellis 1997). The large increase in the quantity of information available on the high-redshift universe at optical wavelengths has

¹Institute of Astronomy, Madingley Road, Cambridge CB3 0HA, UK.

²Space Telescope Science Institute, 3700 San Martin Drive, Baltimore, MD 21218.

³Osservatorio Astronomico di Arcetri, Largo E. Fermi 5, 50125 Firenze, Italy.

been complemented by measurements of the far-IR/sub-mm background by DIRBE and FIRAS onboard the *COBE* satellite (Hauser et al. 1998; Fixsen et al. 1998; Schlegel et al. 1998; Puget et al. 1996), showing that a significant fraction of the energy released by stellar nucleosynthesis is re-emitted as thermal radiation by dust (Dwek et al. 1998), and by theoretical progress made in understanding how intergalactic gas follows the dynamics dictated by dark matter halos until radiative, hydrodynamic, and star formation processes take over (Kauffmann et al. 1993; Baugh et al. 1998; Somerville et al. 1999; Nagamine et al. 1999). Of perhaps equal importance for galaxy formation studies appear the recent findings of the microlensing experiments in the direction of the LMC, which suggest that between 20 and 100% of the dark matter in the Galactic halo is tied up in $0.5^{+0.3}_{-0.2} M_{\odot}$ objects (Alcock et al. 1997). The underlying goal of all these efforts is to understand the growth of cosmic structures, the internal properties of galaxies and their evolution, and ultimately to map the star formation history of the universe from the end of the cosmic ‘dark age’ to the present epoch.

In this paper we focus on the galaxy number-apparent magnitude relation and its first moment, the integrated galaxy contribution to the extragalactic background light (EBL). The logarithmic slope of the differential galaxy counts is a remarkably simple cosmological probe of the history of stellar birth in galaxies, as it must drop below 0.4 to yield a finite value for the EBL. Together with the far-IR/sub-mm background, the optical EBL from both resolved and unresolved extragalactic sources is an indicator of the total luminosity of the universe, as the cumulative emission from young and evolved galactic systems, as well as from active galactic nuclei (AGNs), is recorded in this background. As such it provides, for a given stellar mass function, a quantitative estimate of the baryonic mass that has been processed by stars throughout cosmic history.

Unless otherwise stated, an Einstein-de Sitter (EdS) cosmology ($\Omega_M = 1$, $\Omega_{\Lambda} = 0$) with $H_0 = 100 h \text{ km s}^{-1} \text{ Mpc}^{-1}$ will be adopted in the following. All magnitudes will be given in the AB system.

2. Galaxy counts from UV to near-IR

The HDF-S dataset includes deep near-IR NICMOS images and the deepest observations ever made with the STIS 50CCD imaging mode. The new galaxy sample we use was extracted from version 1 of the HDF-S catalog created with SExtractor (Bertin & Arnout 1996). At near-IR wavelengths it consists of 425 objects detected in the $J + H$ image, over a field of $50'' \times 50''$. The detection threshold was set to $1\sigma_{\text{sky}}$, and the minimum area to 16 drizzled pixels ($0.075''/\text{pxl}$). Magnitudes or upper limits in each band were computed from an area corresponding to the limiting isophote of the $J + H$ image. The 50CCD (corresponding roughly to a $V + I$ filter) STIS catalog consists of 674 objects detected again over a field of $50'' \times 50''$ with a detection threshold of $0.65\sigma_{\text{sky}}$ over 16 drizzled pixel ($0.025''/\text{pxl}$). Details of the data reduction, source detection algorithm, and photometry are can be found on <http://www.stsci.edu/ftp/science/hdfsouth/catalogs.html>.

Figure 1 shows the HDF-N and -S galaxy counts compiled directly from the catalogs, as a function of AB isophotal magnitudes in the $UBVIJHK$ bandpasses for all galaxies with signal-to-noise ratio $S/N > 3$ within the band. No correction for detection completeness have been made; in the HDFs the optical counts are likely to be more than 80% complete down to this limit (Williams et al. 1996). A compilation of existing *HST* and ground-based data is also shown. In addition to our previous compilation (Pozzetti et al. 1998), we have used J and H data from 2MASS (Chester et al. 1998), *HST*/NICMOS (Yan et al. 1998; Teplitz et al. 1998), *NTT*/SOFI (Saracco et al. 1999), and *Keck*/NIRC (Bershady et al. 1998). All magnitudes have been corrected to the AB system, while the second order colour corrections for the differences in the filter effective wavelengths have not been applied to the ground-based data.

One should note that different algorithms used for ‘growing’ the photometry beyond the outer isophotes of galaxies may significantly change the magnitude of faint galaxies. According to Bernstein et al. (1999), roughly 50% of the flux from resolved galaxies with $V > 23$ mag lie outside the standard-sized apertures used by photometric packages. An extragalactic sky pedestal created by the overlapping wings of resolved galaxies also contributes significantly to the sky level, and is undetectable except by absolute surface photometry (Bernstein et al. 1999). Also, at faint magnitude levels, distant objects which are brighter than the nominal depth of the catalog may be missed due to the $(1+z)^4$ dimming factor. All these systematic errors are inherent in faint-galaxy photometry; as a result, our estimates of the integrated fluxes from resolved galaxies will typically be too low, and must be strictly considered as *lower limits*.

3. The brightness of the night sky

The contribution of known galaxies to the optical EBL can be calculated directly by integrating the emitted flux times the differential number counts down to the detection threshold. The results for $0.35 \lesssim \lambda \lesssim 2.2 \mu\text{m}$ are listed in Table 1, along with the magnitude range of integration and the estimated 1σ error bars, which arise mostly from field-to-field variations in the numbers of relatively bright galaxies.

In all seven bands, the slope of the differential number-magnitude relation is flatter than 0.4 above $m_{\text{AB}} \sim 20$ (25) at near-IR (optical) wavelengths, and this flattening appears to be more pronounced at the shorter wavelengths.⁴ The leveling off of the counts is clearly seen in Figure 1, where the function $i_\nu = 10^{-0.4(m_{\text{AB}}+48.6)}N(m)$ is plotted against apparent magnitude in all bands. While counts having a logarithmic slope $d \log N/dm_{\text{AB}} = \alpha \geq 0.40$ continue to add to the EBL at the faintest magnitudes, it appears that the HDF survey has achieved the sensitivity to capture the bulk of the near-ultraviolet, optical, and near-IR extragalactic light from discrete sources. The

⁴A fluctuation analysis by Pozzetti et al. (1998) has shown that the turnover observed in the U band is likely due to the ‘reddening’ of high redshift galaxies caused by neutral hydrogen along the line of sight.

flattening at faint apparent magnitudes cannot be due to the reddening of distant sources as their Lyman break gets redshifted into the blue passband, since the fraction of Lyman-break galaxies at (say) $B \approx 25$ is small (Steidel et al. 1996; Pozzetti et al. 1998). Moreover, an absorption-induced loss of sources cannot explain the similar change of slope of the galaxy counts observed in the V, I, J, H , and K bands. While this suggests that the surface density of optically luminous galaxies is leveling off beyond $z \sim 1.5$, we are worried that a significant amount of light may actually be missed at faint magnitudes because of systematic errors.

The spectrum of the optical EBL is shown in Figure 2, together with the recent results from *COBE*. The value derived by integrating the galaxy counts down to very faint magnitude levels (because of the flattening of the number-magnitude relation most of the contribution to the optical EBL comes from relatively bright galaxies) implies a lower limit to the EBL intensity in the 0.2–2.2 μm interval of $I_{\text{opt}} \approx 15 \text{ nW m}^{-2} \text{ sr}^{-1}$. Including the tentative detection at 3.5 μm by Dwek & Arendt (1999) would boost I_{opt} to $\approx 19 \text{ nW m}^{-2} \text{ sr}^{-1}$. Recent direct measurements of the optical EBL at 3000, 5500, and 8000 \AA from absolute surface photometry by Bernstein et al. (1999) lie between a factor of 2.5 to 3 higher than the integrated light from galaxy counts, with an uncertainty that is largely due to systematic rather than statistical error. Applying this correction factor to the range 3000–8000 \AA gives a total optical EBL intensity in the range $25 - 30 \text{ nW m}^{-2} \text{ sr}^{-1}$. This could become $\sim 45 \text{ nW m}^{-2} \text{ sr}^{-1}$ if the same correction holds also in the near-IR. The *COBE*/FIRAS (Fixsen et al. 1998) measurements yield $I_{\text{FIR}} \approx 14 \text{ nW m}^{-2} \text{ sr}^{-1}$ in the 125–2000 μm range. When combined with the DIRBE (Hauser et al. 1998; Schlegel et al. 1998) points at 140 and 240 μm , one gets a far-IR background intensity of $I_{\text{FIR}}(140 - 2000 \mu\text{m}) \approx 20 \text{ nW m}^{-2} \text{ sr}^{-1}$. The residual emission in the 3.5 to 140 μm region is poorly known, but it is likely to exceed $10 \text{ nW m}^{-2} \text{ sr}^{-1}$ (Dwek et al. 1998). Additional constraints – provided by statistical analyses of the source-subtracted sky – on the EBL have been discussed by, e.g. Martin & Bowyer (1989), Kashlinsky et al. (1996), and Vogeley (1997).

A ‘best-guess’ estimate of the total EBL intensity observed today appears to be

$$I_{\text{EBL}} = 55 \pm 20 \text{ nW m}^{-2} \text{ sr}^{-1}. \quad (1)$$

In the following, we will adopt a reference value for the background light associated with star formation activity over the entire history of the universe of $I_{\text{EBL}} = 50 I_{50} \text{ nW m}^{-2} \text{ sr}^{-1}$.

4. EBL from quasar activity

A direct measurement of the contribution of quasars to the EBL depends on poorly known quantities like the bolometric correction, the faint end of the luminosity function, and the space density of objects at high redshifts. Estimates range from 0.7 to $3 \text{ nW m}^{-2} \text{ sr}^{-1}$ (Soltan 1982; Chokshi & Turner 1992; Small & Blandford 1992). Another source of uncertainty is the possible existence of a distant population of dusty AGNs with strong intrinsic absorption, as invoked in many models for the X-ray background (e.g. Madau et al. 1994; Comastri et al. 1995). These

Type II QSOs, while undetected at optical wavelengths, could contribute significantly to the far-IR background. It is in principle possible to bypass some of the above uncertainties by weighing the local mass density of black holes remnants (Soltan 1982), as recent dynamical evidence indicates that supermassive black holes reside at the center of most nearby galaxies (Richstone et al. 1998). The available data (about 40 objects) show a correlation between bulge and black hole mass, with $M_{\text{BH}} \approx 0.006 M_{\text{sph}}$ as a best-fit (Magorrian et al. 1998). The mass density in old spheroidal populations today is estimated to be $\Omega_{\text{sph}} h = 0.0018^{+0.0012}_{-0.00085}$ (Fukugita et al. 1998, hereafter FHP), implying a mean mass density of quasar remnants today

$$\rho_{\text{BH}} = 3 \pm 2 \times 10^6 h \text{ M}_{\odot} \text{ Mpc}^{-3}. \quad (2)$$

The observed (comoving) energy density from all quasars is equal to the emitted energy, $\eta \rho_{\text{BH}} c^2$, divided by the average quasar redshift, $\langle 1+z \rangle$. Here η is the efficiency of accreted mass to radiation conversion, equal to 5.7% for standard disk accretion onto a Schwarzschild black hole. The total contribution to the EBL from accretion onto black holes can be estimated to be

$$I_{\text{BH}} = \frac{c^3}{4\pi} \frac{\eta \rho_{\text{BH}}}{\langle 1+z \rangle} \approx 4 \pm 2.5 \text{ nW m}^{-2} \text{ sr}^{-1} \frac{\eta}{0.05} \frac{2.5}{\langle 1+z \rangle} \quad (3)$$

($h = 0.5$). Therefore, unless dust-obscured accretion onto supermassive black holes is a very efficient process ($\eta \gg 0.05$), a population of quasars peaking at $z \sim 1.5 - 2$ is expected to make a contribution to the total brightness of the night sky not exceeding 10–20% (Fabian & Iwasawa 1998; Madau 1999).

5. The stellar mass density today

With the help of some simple stellar population synthesis tools we can now set a lower limit to the total stellar mass density that produced the observed EBL, and constrain the cosmic history of star birth in galaxies. One of the most serious uncertainties in this calculation is the lower cutoff, usually treated as a free parameter, of the initial mass function (IMF). Observations of M subdwarfs stars with the *HST* have recently shed some light on this issue, showing that the IMF in the Galactic disk can be represented analytically over the mass range $0.1 < m < 1.6$ (here m is in solar units) by $\log \phi(m) = \text{const} - 2.33 \log m - 1.82(\log m)^2$ (Gould et al. 1996, hereafter GBF; Gould et al. 1997). For $m > 1$ this mass distribution agrees well with a Salpeter function, $\log \phi(m) = \text{const} - 2.35 \log m$. A shallow mass function (relative to the Salpeter slope) below $1 M_{\odot}$ has been measured in the Galactic bulge as well (Zoccali et al. 1999). Observations of normal Galactic star-forming regions also show some convergence in the basic form of the IMF at intermediate and high masses, a power-law slope that is consistent with the Salpeter value (see Elmegreen 1998; Massey 1998, and references therein). In the following we will use a ‘universal’ IMF (shown in Figure 3) with the GBF form for $m < 1$, matched to a Salpeter slope for $m \geq 1$; the mass integral of this function is 0.6 times that obtained extrapolating a Salpeter function down

to $0.1 M_{\odot}$.⁵

As shown in Figure 4, the *bolometric* luminosity as a function of age τ of a simple stellar population (a single generation of coeval, chemically homogeneous stars having total mass M , solar metallicity, and the above IMF) can be well approximated by

$$L(\tau) = \begin{cases} 1200 L_{\odot} \frac{M}{M_{\odot}} & \tau \leq 2.6 \text{ Myr}; \\ 0.7 L_{\odot} \frac{M}{M_{\odot}} \left(\frac{\tau}{1 \text{ Gyr}} \right)^{-1.25} & 2.6 \leq \tau \leq 100 \text{ Myr}; \\ 2.0 L_{\odot} \frac{M}{M_{\odot}} \left(\frac{\tau}{1 \text{ Gyr}} \right)^{-0.8} & \tau > 100 \text{ Myr} \end{cases} \quad (4)$$

(cf Buzzoni 1995). Over a timescale of 13 Gyr (the age of the universe for an EdS cosmology with $h = 0.5$), about 1.3 MeV per stellar baryon will be radiated away. This number depends only weakly on the assumed metallicity of stars. In a stellar system with arbitrary star formation rate per comoving cosmological volume, $\dot{\rho}_s$, the bolometric emissivity at time t is given by the convolution integral

$$\rho_{\text{bol}}(t) = \int_0^t L(\tau) \dot{\rho}_s(t - \tau) d\tau. \quad (5)$$

Therefore the total background light observed at Earth ($t = t_H$), generated by a stellar population with a formation epoch t_F , is

$$I_{\text{EBL}} = \frac{c}{4\pi} \int_{t_F}^{t_H} \frac{\rho_{\text{bol}}(t)}{1+z} dt, \quad (6)$$

where the factor $(1+z)$ at the denominator is lost to cosmic expansion when converting from observed to radiated (comoving) luminosity density.

To set a lower limit to the present-day mass density, Ω_{g+s} , of processed gas + stars (in units of the critical density $\rho_{\text{crit}} = 2.77 \times 10^{11} h^2 M_{\odot} \text{Mpc}^{-3}$), consider now a scenario where all stars are formed *instantaneously* at redshift z_F . The background light that would be observed at Earth from such an event is shown in Figure 4 as a function of z_F for $\Omega_{g+s} h^2 = 0.0008, 0.0013, 0.0018$, corresponding to 4, 7, and 9 percent of the nucleosynthetic baryon density, $\Omega_b h^2 = 0.0193 \pm 0.0014$ (Burles & Tytler 1998). Two main results are worth stressing here: (1) the time evolution of the luminosity radiated by a simple stellar population (eq. 4) makes the dependence of the observed EBL from z_F much shallower than the $(1+z_F)^{-1}$ lost to cosmic expansion (eq. 6), as the energy output from stars is spread over their respective lifetimes; and (2) in order to generate an EBL at a level of $50 I_{50} \text{ nW m}^{-2} \text{sr}^{-1}$, one requires $\Omega_{g+s} h^2 > 0.0013 I_{50}$ for an EdS universe with $h = 0.5$, hence a mean mass-to-blue light ratio today of $\langle M/L_B \rangle_{g+s} > 3.5 I_{50}$ (the total blue luminosity density at the present-epoch is $\mathcal{L}_B = 2 \times 10^8 h L_{\odot} \text{Mpc}^{-3}$, Ellis et al. 1996). The dependence of these estimates on the cosmological model (through eq. 6) is rather weak. With the adopted IMF,

⁵The bolometric light contributed by stars less massive than $1 M_{\odot}$ is very small for a ‘typical’ IMF. The use of the GBF mass function at low masses instead of Salpeter then leaves the total radiated luminosity of a stellar population virtually unaffected.

about 30% of this mass will be returned to the interstellar medium in 10^8 yr, after intermediate-mass stars eject their envelopes and massive stars explode as supernovae. This return fraction, R , becomes 50% after about 10 Gyr.⁶

A visible mass density at the level of the above lower limit, while able to explain the measured sky brightness, requires (most of the stars) that give origin to the observed light to have formed at very low redshifts ($z_F \lesssim 0.5$), a scenario which appears to be ruled out by the observed evolution of the UV luminosity density (Madau 1999). For illustrative purposes, it is interesting to consider instead a model where the star formation rate per unit comoving volume stays approximately constant with cosmic time. In an EdS cosmology with $h = 0.5$, one derives from equations (4), (5), and (6)

$$I_{\text{EBL}} = 1460 \text{ nW m}^{-2} \text{ sr}^{-1} \langle \frac{\dot{\rho}_s}{\text{M}_\odot \text{ yr}^{-1} \text{ Mpc}^{-3}} \rangle. \quad (7)$$

The observed EBL therefore implies a ‘fiducial’ mean star formation density of $\langle \dot{\rho}_s \rangle = 0.034 I_{50} \text{ M}_\odot \text{ yr}^{-1} \text{ Mpc}^{-3}$ (or a factor of 1.6 higher in the case of a Salpeter IMF down to $0.1 M_\odot$). Any value much greater than this over a sizeable fraction of the Hubble time will generate an EBL intensity well in excess of $50 \text{ nW m}^{-2} \text{ sr}^{-1}$. Ignoring for the moment the recycling of returned gas into new stars, the visible mass density at the present epoch is simply $\rho_{g+s} = \int_0^{t_H} \dot{\rho}_s(t) dt = 4.4 \times 10^8 I_{50} \text{ M}_\odot \text{ Mpc}^{-3}$, corresponding to $\Omega_{g+s} h^2 = 0.0016 I_{50}$ ($\langle M/L_B \rangle_{g+s} = 4.4 I_{50}$).

Perhaps a more realistic scenario is one where the star formation density evolves as

$$\dot{\rho}_s(z) = \frac{0.23 e^{3.4z}}{e^{3.8z} + 44.7} \text{ M}_\odot \text{ yr}^{-1} \text{ Mpc}^{-3}. \quad (8)$$

This fits reasonably well all measurements of the UV-continuum and $\text{H}\alpha$ luminosity densities from the present-epoch to $z = 4$ after an extinction correction of $A_{1500} = 1.2 \text{ mag}$ ($A_{2800} = 0.55 \text{ mag}$) is applied to the data (Madau 1999), and produce a total EBL of about the right magnitude ($I_{50} \approx 1$). Since about half of the present-day stars are formed at $z > 1.3$ in this model and their contribution to the EBL is redshifted away, the resulting visible mass density is $\Omega_{g+s} h^2 = 0.0031 I_{50}$ ($\langle M/L_B \rangle_{g+s} = 8.6 I_{50}$), almost twice as large as in the $\dot{\rho}_s = \text{const}$ approximation.

We conclude that, depending on the star formation history and for the assumed IMF, the observed EBL requires between 7% and 16% of the nucleosynthetic baryon density to be today in the forms of stars, processed gas, and their remnants. According to the most recent census of cosmic baryons, the mass density in stars and their remnants observed today is $\Omega_s h = 0.00245^{+0.00125}_{-0.00088}$ (FHP), corresponding to a mean stellar mass-to-blue light ratio of $\langle M/L_B \rangle_s = 3.4^{+1.7}_{-1.3}$ for $h = 0.5$ (roughly 70% of this mass is found in old spheroidal populations). While this is about a factor of 2.5 smaller than the visible mass density predicted by equation (8), efficient recycling of ejected

⁶An asymptotic mass fraction of stars returned as gas, $R = \int (m - m_f) \phi(m) dm \times [\int m \phi(m) dm]^{-1} \approx 0.5$, can be obtained by using the semiempirical initial (m)–final (m_f) mass relation of Weidemann (1987) for stars with $1 < m < 10$, and by assuming that stars with $m > 10$ return all but a $1.4 M_\odot$ remnant.

material into new star formation would tend to reduce the apparent discrepancy in the budget. Alternatively, the gas returned by stars may be ejected into the intergalactic medium. With an IMF-averaged yield of returned metals of $y_Z \approx 1.5 Z_\odot$,⁷ the predicted mean metallicity at the present epoch is $y_Z \Omega_{g+s} / \Omega_b \approx 0.25 Z_\odot$, in good agreement with the values inferred from cluster abundances (Renzini 1997).

6. EBL from MACHOs

One of the most interesting constraints posed by the observed brightness of the night sky concerns the possibility that a large fraction of the dark mass in present-day galaxy halos may be associated with faint white-dwarf (WD) remnants of a population of intermediate-mass stars that formed at high redshifts. The results of the microlensing MACHO experiment towards the LMC indicates that $60 \pm 20\%$ of the sought dark matter in the halo of the Milky Way may be in the form of $0.5^{+0.3}_{-0.2} M_\odot$ objects (Alcock et al. 1997). The mass scale is a natural one for white dwarfs, a scenario also supported by the lack of a numerous spheroidal population of low-mass main sequence stars in the HDF (Gould et al. 1998). The total mass of MACHOs inferred within 50 kpc is $2^{+1.2}_{-0.7} \times 10^{11} M_\odot$, implying a ‘MACHO-to-blue light’ ratio for the Milky Way in the range 5 to 25 solar (cf Fields et al. 1998). If these values were typical of the luminous universe as a whole, i.e. if MACHOs could be viewed as a new stellar population having similar properties in all disk galaxies, then the cosmological mass density of MACHOS today would be $\Omega_{\text{MACHO}} = (5 - 25) f_B \mathcal{L}_B / \rho_{\text{crit}} = (0.0036 - 0.017) f_B h^{-1}$, a significant entry in the cosmic baryon budget (Fields et al. 1998). Here $f_B \approx 0.5$ is the fraction of the blue luminosity density radiated by stellar disks (FHP). Note that if MACHOs are halo WDs, the contribution of their progenitors to the mass density parameter is several times higher.

Halo IMFs which are very different from that of the solar neighborhood, i.e. which are heavily-biased towards WD progenitors and have very few stars forming with masses below $2 M_\odot$ (as these would produce bright WDs in the halo today that are not seen), and above $8 M_\odot$ (to avoid the overproduction of heavy elements), have been suggested as a suitable mechanism for explaining the microlensing data (Adams & Laughlin 1996; Chabrier et al. 1996). While the halo WD scenario may be tightly constrained by the observed rate of Type Ia SN in galaxies (Smecker & Wyse 1991), the expected C and N overenrichment of halo stars (Gibson & Mould 1997), and the number counts of faint galaxies in deep optical surveys (Charlot & Silk 1995), here we explore a potentially more direct method (as it does not depend on, e.g. extrapolating stellar yields to primordial metallicities, on galactic winds removing the excess heavy elements into the intergalactic medium, or on the reddening of distant halos by dust), namely we will compute the contribution of WD progenitors in dark galaxy halos to the extragalactic background light.

⁷Here we have taken $y_Z \equiv \int m p_{\text{zm}} \phi(m) dm \times [\int m \phi(m) dm]^{-1}$, the stellar yields p_{zm} of Tsujimoto et al. (1995), and a GBF+Salpeter IMF.

Following Chabrier (1999), we adopt a truncated power-law IMF,

$$\phi(m) = \text{const} \times e^{-(\overline{m}/m)^3} m^{-5}. \quad (9)$$

This form mimics a mass function strongly peaked at $0.84\overline{m}$. To examine the dependence of the IMF on the results we consider two functions (shown in Fig. 3), $\overline{m} = 2.4$ and $\overline{m} = 4$: both yield a present-day Galactic halo mass-to-light ratio > 100 after a Hubble time, as required in the absence of a large non-baryonic component. We further assume that a population of halo WD progenitors having mass density $X\Omega_b h^2 = 0.0193X$ formed instantaneously at redshift z_F with this IMF and nearly primordial ($Z = 0.02 Z_\odot$) metallicity. The resulting EBL from such an event is huge, as shown in Figure 5 for $X = 0.1, 0.3$, and 0.6 and a Λ -dominated universe with $\Omega_M = 0.3$, $\Omega_\Lambda = 0.7$, and $h = 0.65$ ($t_H = 14.5$ Gyr).

Consider the $\overline{m} = 2.4$ case first. With $z_F = 3$ and $X = 0.6$, this scenario would generate an EBL at a level of $300 \text{ nW m}^{-2} \text{ sr}^{-1}$. Even if only 30% of the nucleosynthetic baryons formed at $z_F = 5$ with a WD-progenitor dominated IMF, the resulting background light at Earth would exceed the value of $100 \text{ nW m}^{-2} \text{ sr}^{-1}$, the ‘best-guess’ upper limit to the observed EBL from the data plotted in Figure 2. The return fraction is $R \approx 0.8$, so only 20% of this stellar mass would be leftover as WDs, the rest being returned to the ISM. Therefore, if galaxy halos comprise 100% of the nucleosynthetic baryons, only a small fraction of their mass, $X_{\text{WD}} \approx 0.2 \times 0.30 = 0.06$ could be in the form of white dwarfs. Pushing the peak of the IMF to more massive stars, $\overline{m} = 4$, helps only marginally. With $\overline{m} = 2.4$, the energy radiated per stellar baryon over a timescale of 13 Gyr is equal to 2 MeV, corresponding to 10 MeV per baryon in WD remnants. A similar value is obtained in the $\overline{m} = 4$ case: because of the shorter lifetimes of more massive stars the expected EBL is reduced, but only by 20% or so (see Fig. 5). Moreover, the decreasing fraction of leftover WDs raises even more severe problems of metal galactic enrichment.

Note that these limits are not necessarily in contrast with the microlensing results, as they may imply either that WDs are not ubiquitous in galaxy halos (i.e. the Milky Way is atypical), or that the bulk of the baryons are actually not galactic. One possible way to relax the above constraints on WD baryonic halos is to push their formation epoch to extreme redshifts ($z_F > 10$), and hide the ensuing background light in the poorly constrained spectral region between 5 and $100 \mu\text{m}$. In Figure 2 we show the EBL produced by a WD-progenitor dominated IMF with $\overline{m} = 4$ and $(z_F, X, X_{\text{WD}}) = (36, 0.5, 0.1)$, assuming negligible dust reddening. While this model may be consistent with the observations if the large corrections factors inferred by Bernstein et al. (1999) extend into the near-IR, we draw attention to the fact that even a tiny fraction of dust reprocessing in the (redshifted) far-IR would inevitably lead to a violation of the FIRAS background.

We have benefited from useful discussions with R. Bernstein, G. Bruzual, C. Hogan, A. Loeb, and G. Zamorani. We are indebted to R. Bernstein, W. Freedman, & B. Madore for communicating their unpublished results on the EBL. Partial support for this work was provided by NASA through grant AR-06337.10-94A from the Space Telescope Science Institute.

REFERENCES

- Alcock, C., et al. 1997, *ApJ*, 486, 697
- Armand, C., Milliard, B., & Deharveng, J.-M. 1994, *A&A*, 284, 12
- Baugh, C. M., Cole, S., Frenk, C. S., & Lacey, C. G. 1998, *ApJ*, 498, 504
- Bernstein, R. A., Freedman, W. L., & Madore, B. F. 1999, preprint
- Bershady, M. A., Lowenthal, J. D., & Koo, D. C. 1998, *ApJ*, 505, 50
- Bertin, E., & Arnouts, S. 1996, *A&AS*, 117, 393
- Bruzual, A. C., & Charlot, S. 1993, *ApJ*, 405, 538
- Burles, S., & Tytler, D. 1998, *ApJ*, 499, 699
- Buzzoni, A. 1995, *ApJS*, 98, 69
- Chabrier, G. 1999, *ApJ*, in press (astro-ph/9901145)
- Chabrier, G., Segretain, L., & Mera, D. 1996, *ApJ*, 468, L21
- Charlot, S., & Silk, J. 1995, *ApJ*, 445, 124
- Chester, T., Jarret, T., Schneider, S., Skrutskie, M., & Huchra, J. 1998, *AAS*, 192, 5511
- Chokshi, A., & Turner, E. L. 1992, *MNRAS*, 259, 421
- Comastri, A., et al. 1995, *A&A*, 296, 1
- Dwek, E., & Arendt, R. G. 1999, *ApJ*, in press (astro-ph/9809239)
- Dwek, E., et al. 1998, *ApJ*, 508, 106
- Elbaz, D., et al. 1998, in *The Universe as seen by ISO*, ed. P. Cox & M. F. Kessler (Noordwijk: ESA Pub.), in press (astro-ph/9902229)
- Ellis, R. S. 1997, *ARA&A*, 35, 389
- Ellis, R. S., Colless, M., Broadhurst, T., Heyl, J., & Glazebrook, K. 1996, *MNRAS*, 280, 235
- Elmegreen, B. G. 1998, in *Unsolved Problems in Stellar Evolution*, ed. M. Livio (Cambridge: Cambridge University Press), in press (astro-ph/9811289)
- Fabian, A. C., & Iwasawa, K. 1999, *MNRAS*, in press
- Fields, B.D., Freese, K., & Graff, D. S. 1998, *NewA*, 3, 347
- Fixsen, D. J., et al. 1998, *ApJ*, 508, 123
- Fukugita, M., Hogan, C. J., & Peebles, P. J. E. 1998, *ApJ*, 503, 518
- Gibson, B., & Mould, J. 1997, *ApJ*, 482, 98
- Gould, A., Bahcall, J. N., & Flynn, C. 1996, *ApJ*, 465, 759 (GBF)
- Gould, A., Bahcall, J. N., & Flynn, C. 1997, *ApJ*, 482, 913
- Gould, A., Flynn, C., & Bahcall, J. N. 1998, *ApJ*, 503, 798

- Hauser, M. G., et al. 1998, *ApJ*, 508, 25
- Kashlinsky, A., Mather, J. C., Odenwald, S., & Hauser, M. G. 1996, *ApJ*, 470, 681
- Kauffmann, G., White, S. D. M., & Guiderdoni, B. 1993, *MNRAS*, 264, 201
- Lagache, G., Abergel, A., Boulanger, F., Desert, F. X., & Puget, J.-L. 1999, *A&A*, 344, 322
- Madau, P. 1999, in *Proceedings of the Nobel Symposium on Particle Physics and the Universe*, *Physica Scripta*, in press
- Madau, P., Ghisellini, G., & Fabian, A. C. 1994, *MNRAS*, 270, L17
- Madau, P., Pozzetti, L., & Dickinson, M. 1998, *ApJ*, 498, 106
- Magorrian, G., et al. 1998, *AJ*, 115, 2285
- Martin, C., & Bowyer, S. 1989, *ApJ*, 338, 677
- Massey, P. 1998, in *The Stellar Initial Mass Function*, ed. G. Gilmore & D. Howell (San Francisco: ASP), p. 17
- Nagamine, K., Cen, R., & Ostriker, J. P. 1999, *ApJ*, submitted (astro-ph/9902372)
- Pozzetti, L., Madau, P., Zamorani, G., Ferguson, H. C., & Bruzual, A. G. 1998, *MNRAS*, 298, 1133
- Puget, J.-L., Abergel, A., Bernard, J.-P., Boulanger, F., Burton, W. B., Desert, F.-X., & Hartmann, D. 1996, *A&A*, 308, L5
- Renzini, A. 1997, *ApJ*, 488, 35
- Richstone, D., et al. 1998, *Nature*, 395, 14
- Saracco, P., D’Odorico, S., Moorwood A., & Cuby, J. G. 1999, *Ap&SS*, in press (astro-ph/9904069)
- Schlegel, D. J., Finkbeiner, D. P., & Davis, M. 1998, *ApJ*, 500, 525
- Small, T. D., & Blandford, R. D. 1992, *MNRAS*, 259, 725
- Smecker, T. A., & Wyse, R. 1991, *ApJ*, 372, 448
- Soltan, A. 1982, *MNRAS*, 200, 115
- Somerville, R. S., Primack, J. R., & Faber, S. M. 1999, *MNRAS*, in press (astro-ph/9802268)
- Steidel, C. C., Adelberger, K., Dickinson, M. E., Giavalisco, M., & Pettini, M. 1998, in *The Birth of Galaxies*, ed. B. Guiderdoni, F. R. Bouchet, Trinh X. Thuan, & Tran Thanh Van (Gif-sur-Yvette: Edition Frontieres), in press (astro-ph/9812167)
- Steidel, C. C., Giavalisco, M., Pettini, M., Dickinson, M. E., & Adelberger, K. 1996, *ApJ*, 462, L17
- Teplitz, H. I., Gardner, J. P., Malumuth, E. M., & Heap, S. R. 1998, *ApJ*, 507, L17
- Tsujimoto, T., Nomoto, K., Yoshii, Y., Hashimoto, M., Yanagida, S., & Thielemann, F.-K. 1995, *MNRAS*, 277, 945
- Vogeley, M. S. 1997, *AAS*, 191, 304
- Weidemann, V. 1987, *A&A*, 188, 74

Williams, R. E., et al. 1996, *AJ*, 112, 1335

Yan, L., McCarthy, P. J., Storrie-Lombardi, L. J., & Weymann, R. J. 1998, *ApJ*, 503, L19

Zoccali, M., et al. 1999, *ApJ*, submitted (astro-ph/9906452)

Table 1. Integrated Galaxy Light

λ (Å)	AB (range)	νI_ν	σ^+	σ^-
3600	18.0–28.0	2.87	0.58	0.42
4500	15.0–29.0	4.57	0.73	0.47
6700	15.0–30.5	6.74	1.25	0.94
8100	12.0–29.0	8.04	1.62	0.92
11000	10.0–29.0	9.71	3.00	1.90
16000	10.0–29.0	9.02	2.62	1.68
22000	12.0–25.5	7.92	2.04	1.21

Note. — νI_ν is in units of $\text{nW m}^{-2} \text{sr}^{-1}$.

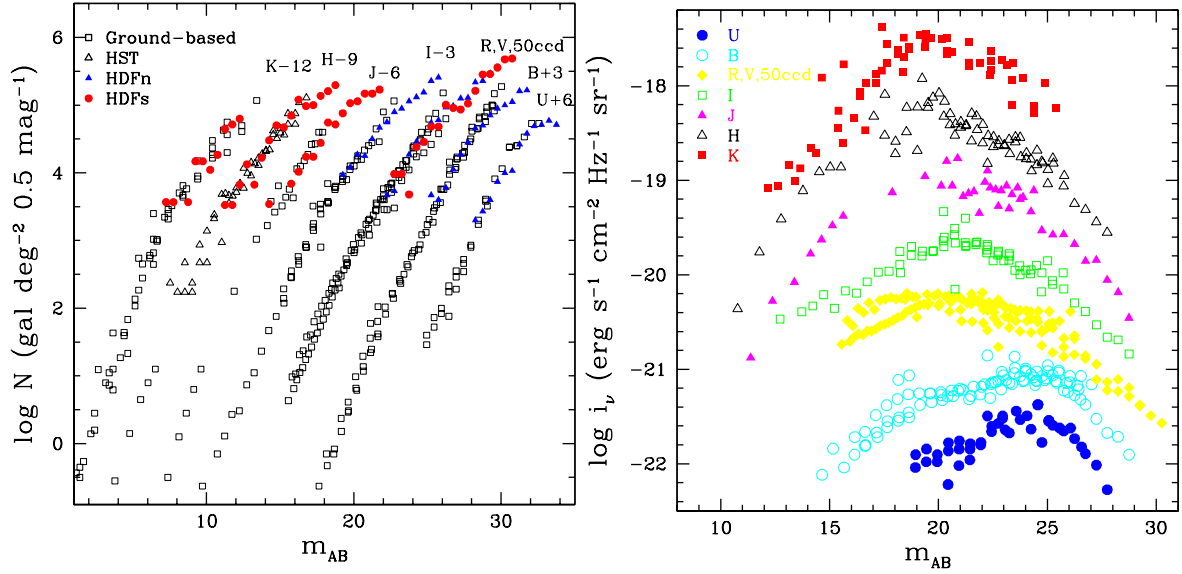


Fig. 1.— *Left*: Differential $UBVIJHK$ galaxy counts as a function of AB magnitudes. The sources of the data points are given in the text. Note the decrease of the logarithmic slope $d \log N / dm$ at faint magnitudes. The flattening is more pronounced at the shortest wavelengths. *Right*: Extragalactic background light per magnitude bin, $i_\nu = 10^{-0.4(m_{\text{AB}} + 48.6)} N(m)$, as a function of U (filled circles), B (open circles), V (filled pentagons), I (open squares), J (filled triangles), H (open triangles), and K (filled squares) magnitudes. For clarity, the $BVIJHK$ measurements have been multiplied by a factor of 2, 6, 15, 50, 150, and 600, respectively.

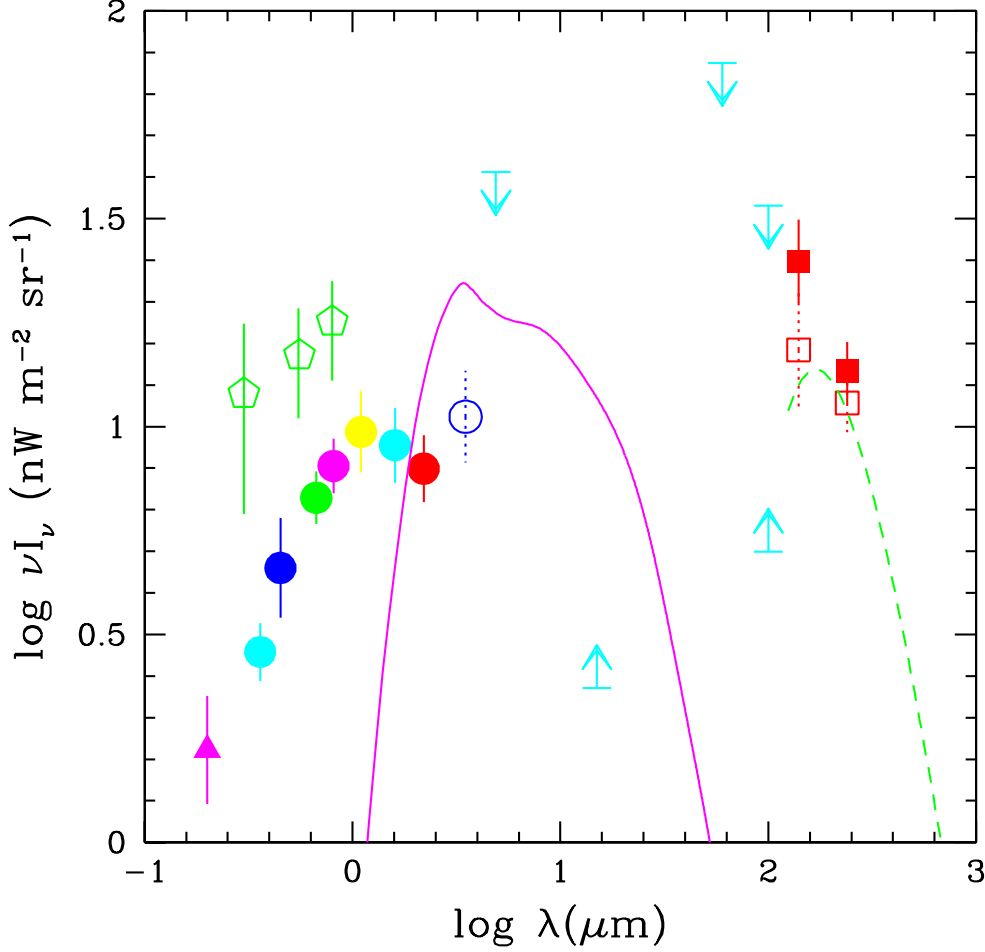


Fig. 2.— Spectrum of the optical extragalactic background light from resolved sources as derived from a compilation of ground-based and space-based galaxy counts in the $UBVIJHK$ bands (*filled dots*), together with the FIRAS 125–5000 μm (*dashed line*) and DIRBE 140 and 240 μm (*filled squares*) detections (Hauser et al. 1998; Fixsen et al. 1998). The *empty squares* show the DIRBE points after correction for WIM dust emission (Lagache et al. 1999). Also plotted (*filled triangle*) is a FOCA-UV point at 2000 \AA from Armand et al. (1994), and a tentative detection at 3.5 μm (*empty dot*) from *COBE*/DIRBE observations (Dwek & Arendt 1999). The empty pentagons at 3000, 5500, and 8000 \AA are Bernstein et al. (1999) measurements of the EBL from resolved and unresolved galaxies fainter than $V = 23$ mag (the error bars showing 2σ statistical errors). Upper limits are from Hauser et al. (1998), the lower limit from Elbaz et al. (1999). The *solid curve* shows the synthetic EBL produced by a WD-progenitor dominated IMF with $\overline{m} = 4$ and $(z_F, X, X_{\text{WD}}) = (36, 0.5, 0.1)$, in the case of zero dust reddening.

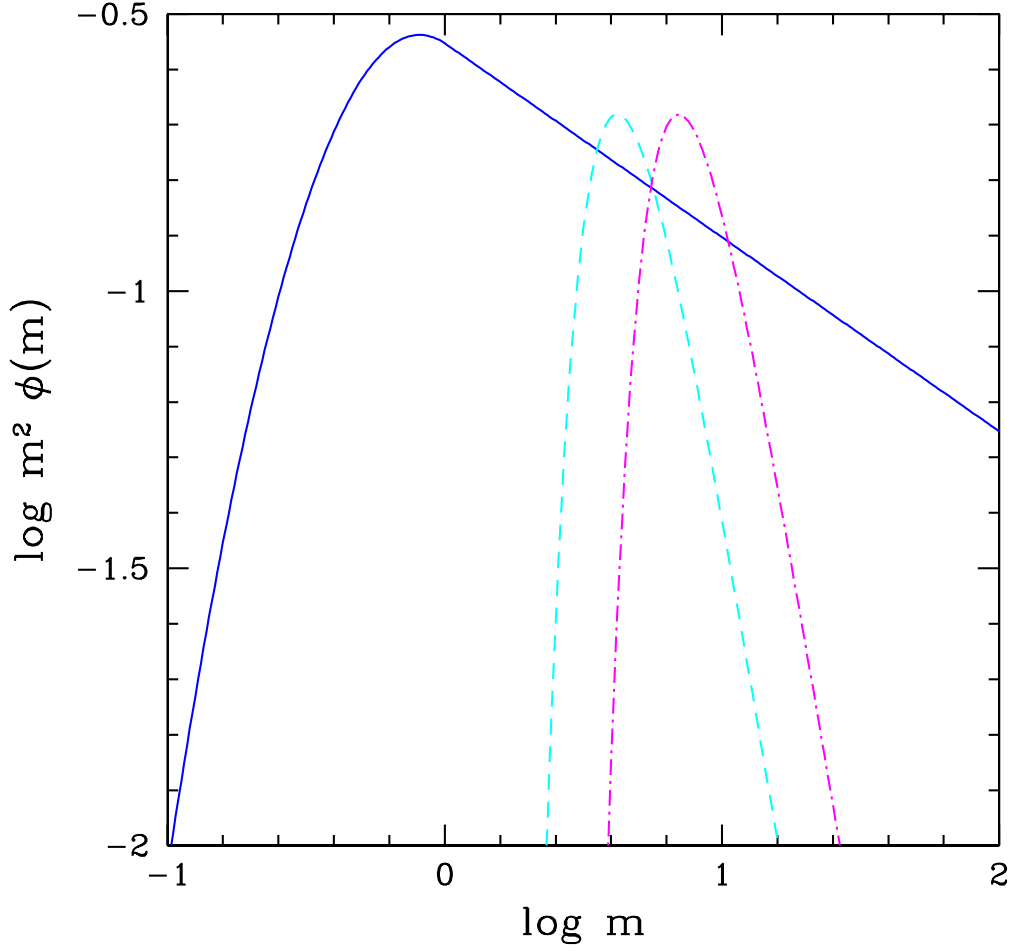


Fig. 3.— Stellar initial mass functions, $\phi(m)$, multiplied by m^2 . *Solid line*: Salpeter IMF, $\phi(m) \propto m^{-2.35}$ at high masses, matched to a GBF function at $m \leq 1$. *Dotted line*: WD-progenitor dominated IMF in galaxy halos, $\phi(m) \propto e^{-(\overline{m}/m)^3} m^{-5}$, with $\overline{m} = 2.4$ (see text for details). *Dot-dashed line*: Same for $\overline{m} = 4$. All IMFs have been normalized to $\int m\phi(m)dm = 1$.

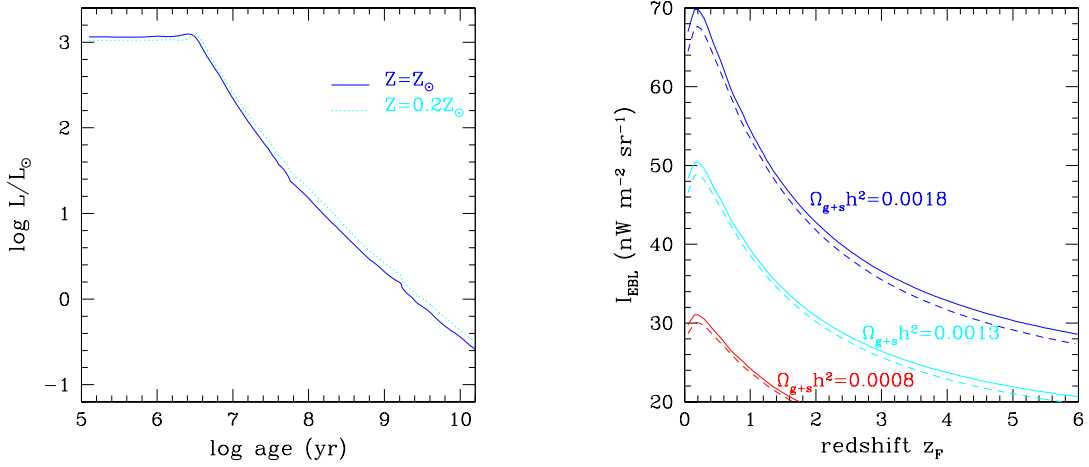


Fig. 4.— *Left*: Synthetic (based on an update of Bruzual & Charlot’s 1993 libraries) bolometric luminosity versus age of a simple stellar population having total mass $M = 1 M_\odot$, metallicity $Z = Z_\odot$ (*solid line*) and $Z = 0.2 Z_\odot$ (*dotted line*), and a GBF+Salpeter IMF (see text for details). *Right*: EBL observed at Earth from the instantaneous formation at redshift z_F of a stellar population having the same IMF ($Z = Z_\odot$) and mass density $\Omega_{g+s}h^2 = 0.0018, 0.0013$, and 0.0008 , as a function of z_F . *Solid curves*: EdS universe with $h = 0.5$ ($t_H = 13$ Gyr). *Dashed curves*: Λ -dominated universe with $\Omega_M = 0.3$, $\Omega_\Lambda = 0.7$, and $h = 0.65$ ($t_H = 14.5$ Gyr).

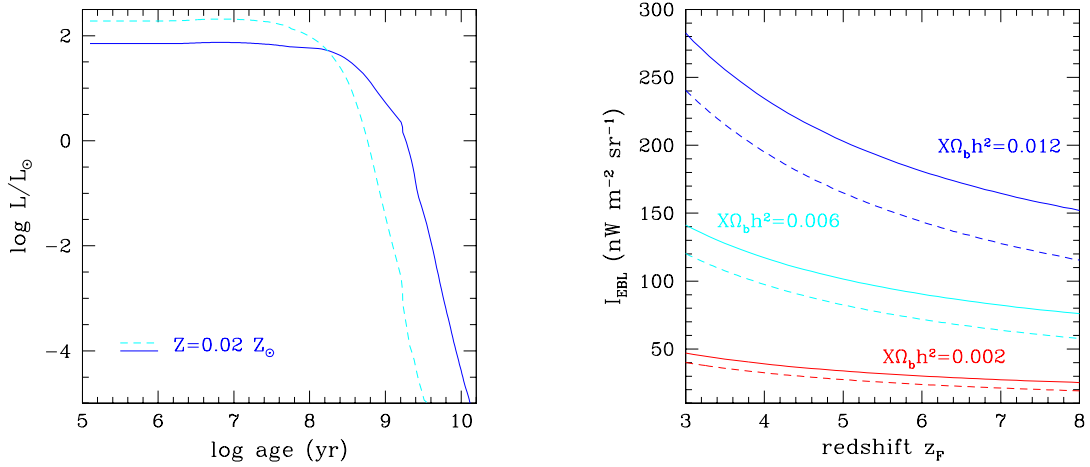


Fig. 5.— *Left:* Synthetic bolometric luminosity versus age of a simple stellar population having total mass $M = 1 M_\odot$, metallicity $Z = 0.02 Z_\odot$, and a WD-progenitor dominated IMF (see text for details) with $\overline{m} = 2.4$ (*solid line*) and $\overline{m} = 4$ (*dashed line*). *Right:* EBL observed at Earth from the instantaneous formation at redshift z_F of a stellar population having the same IMF and metallicity, and mass density $X\Omega_b h^2 = 0.012, 0.006$ and 0.002 (corresponding to 60, 30, and 10 per cent of the nucleosynthetic value), as a function of z_F . A Λ -dominated universe with $\Omega_M = 0.3$, $\Omega_\Lambda = 0.7$, and $h = 0.65$ has been assumed. *Solid line:* $\overline{m} = 2.4$. *Dashed line:* $\overline{m} = 4$.